



Article

Numerical Simulation of Soliton Propagation Behavior for the Fractional-in-Space NLSE with Variable Coefficients on Unbounded Domain

Fengzhou Tian ¹, Yulan Wang ^{2,*} and Zhiyuan Li ³

¹ School of Mathematics and Statistics, Northeastern University, Qinhuangdao 066004, China; 13039505118@163.com

² Department of Mathematics, Inner Mongolia University of Technology, Hohhot 010051, China

³ College of Date Science and Application, Inner Mongolia University of Technology, Hohhot 010080, China; lizhiyuan2064@imut.edu.cn

* Correspondence: wylnei@imut.edu.cn

Abstract: The soliton propagation of the fractional-in-space nonlinear Schrodinger equation (NLSE) is much more complicated than that of the corresponding integer NLSE. The aim of this paper is to discover some novel fractal soliton propagation behaviors (FSPBs) of this fractional-in-space NLSE. Firstly, the exact solution is compared with the present numerical solution, and the validity and accuracy of the present numerical method are verified. Secondly, the effect of fractional derivatives on soliton propagation is explored through the present numerical simulation results. At the same time, the present method is extended to the three-dimensional fractional-order NLSE. Finally, some novel FSPBs of the fractional-in-space NLSE are given.

Keywords: fractional NLSE; soliton propagation; unbounded domain; numerical simulation



Citation: Tian, F.; Wang, Y.; Li, Z. Numerical Simulation of Soliton Propagation Behavior for the Fractional-in-Space NLSE with Variable Coefficients on Unbounded Domain. *Fractal Fract.* **2024**, *8*, 163. <https://doi.org/10.3390/fractalfract8030163>

Academic Editors: Jaroslaw Krzywanski, Marcin Sosnowski, Karolina Grabowska, Dorian Skrobek, Ghulam Moeen Uddin and Carlo Cattani

Received: 18 February 2024

Revised: 7 March 2024

Accepted: 9 March 2024

Published: 12 March 2024



Copyright: © 2024 by the authors. Licensee MDPI, Basel, Switzerland. This article is an open access article distributed under the terms and conditions of the Creative Commons Attribution (CC BY) license (<https://creativecommons.org/licenses/by/4.0/>).

1. Introduction

The following fractional-in-space NLSE is considered [1–3]

$$\begin{cases} i \frac{\partial \mathbf{u}(x,t)}{\partial t} - d_1(t) \frac{\partial \mathbf{u}(x,t)}{\partial x} + id_2(t) \Delta^{\frac{\alpha}{2}} \mathbf{u}(x,t) + d_3(t) \mathbf{u}(x,t) |\mathbf{u}(x,t)|^2 = 0, (x,t) \in \mathbb{R} \times [0, T], \\ \mathbf{u}(x,0) = \mathbf{u}_0(x), x \in \mathbb{R}, \\ |\mathbf{u}(x,t)| \rightarrow 0, |x| \rightarrow \infty, 0 < t \leq T, \end{cases} \quad (1)$$

where three variable coefficients $d_1(t)$, $d_2(t)$, $d_3(t)$ are known functions, $\mathbf{u}_0(x)$ is a known functions and is called the initial condition, and this complex-valued function $\mathbf{u}(x,t)$ is an unknown. $i = \sqrt{-1}$, $\Delta^{\frac{\alpha}{2}} \mathbf{u}(x,t)$ is the Laplacian operator with the Riesz fractional-in-space derivative.

In order to investigate the dynamic behavior of the NLSE, a number of scholars studied the numerical solution of the NLSE. The finite difference scheme is a commonly used numerical method, and the finite difference scheme [4] is used to simulate the weakly damping NLSE [5], the NLSE with a damping term [6], time-space-fractional NLSE [7], and generalized NLSE [8]. Zhang [8] employed the shifted and weighted Grünwald difference scheme to approximate the Riesz fractional-in-space derivative and the $L2 - 1_\sigma$ scheme to approximate the Caputo fractional-in-time derivative. Liu and Ran constructed an arbitrarily order energy conserving finite difference scheme [9] for the fractional-in-time generalized NLSE. Yuan et al. [10] presented a general linearized difference scheme for numerically solving the fractional-in-time-space NLSE by using the fast variable-step $L2 - 1_\sigma$ approach, the linearized method [11] is developed to discrete time variables, and the Fourier spectral method (FSM) is applied to discrete spatial variables. Li and Chen [12] constructed an artificial boundary method to study the dynamic behavior of the NLSE in an unbounded domain with a damping term. The main advantage of this approach is that

an efficient transformation is applied to eliminate the damping term. Cai and Chen [13] combined the Runge-Kutta method (RKM), the integral factor method, and the supplementary variable method to propose a prediction-correction scheme to study the dynamic behavior of the NLSE with fractional-in-space Laplacian operators [14]. Cai et al. [15] adopted the dissipation-preserving Galerkin approach to numerically solve the space fractional order NLSE with a strongly damping term. The differential quadrature method is applied by Ali et al. [16] to numerically solve the NLSE. The sinc function is developed by Moritz Braun [17], and the scaled and shifted sinc functions on a finite interval are given. Moritz Braun [17] numerically solved the one-dimensional fractional-order NLSE. A semiclassical method is used by Kulagin and Shapovalov [18] to solve the NLSE with a non-Hermitian term. Aldhaferi and Nuwairan [19] gave some solutions for the fractional-in-time-modified NLSE. Muhammad et al. [20] combined the compelling homotopy perturbation method [21] with the conformable natural transform technique for obtaining some numerical and analytical solutions of the fractional-in-time NLSE with trapping potential. Authors utilized the famous Crank-Nicolson scheme for time derivatives of the standard Boussinesq equation, while a standard spectral scheme for the NLSE is applied.

The spectral method is also one of the numerical methods often used by scholars. It is essentially an extension of the standard variable separation technique. Chebyshev polynomials and Legendre polynomials are usually chosen as basis functions. For periodic boundary conditions, it is convenient to use Fourier series and harmonic series. The accuracy of the spectral method depends directly on the number of terms of the series expansion. The idea of the FSM is as follows: Firstly, the fast Fourier transform (FFT) for the partial differential equation is carried out to obtain ordinary differential equations. Then, a numerical scheme is used to solve these ordinary differential equations. In [22], the Crank-Nicolson FSM is given for the space fractional standard NLSE. The FFT is applied to practical computation and the famous Crank-Nicolson scheme for time derivatives. Abdolabadi [23] presented the FSM for solving the fractional-in-space NLSE by using the pseudo-FSM [24] in the general Riesz fractional-in-space derivative. In [25], the time-splitting FSM is developed to study the coupled nonlinear standard Schrödinger–Boussinesq equations. In [26], a fourth-order exponential FSM has been given for the fractional-in-space compelling NLSE. This method is the fourth-order exponential-difference approach for time derivatives. The FFT technique is used for a spatial variable. Farag et al. [27] applied three spectral difference methods, namely the split-step FSM, the FSM, and the hopscotch approach, to provide an effective numerical solution for the (2+1)-dimensional NLSE. In [28], authors developed a regularized Lie-Trotter splitting FSM to study the fractional-in-space regularized logarithmic NLSE. Wang et al. [29,30] have used the FSM to investigate a class of fraction-in-space standard KdV-modified KdV equations and fractional reaction-diffusion models. It should be noted that the FSM generally defaults its boundary condition to a periodic boundary; that is, the function value at one end of the boundary will affect the function value at the other end of the boundary. For some aperiodic boundary condition problems, how to ensure that the value at the boundary has little effect on the whole or that the value at the boundary is always a specific constant is a problem worth thinking about.

The goal of this paper is to discover some novel FSPBs of the NLSE with variable coefficients on an unbounded domain by developing FFT and RKM.

2. Description of Method

The method is meant to employ the compelling FFT for spatial variables and to use the RKM for time derivatives. This method is spectral-convergent in space and three-order-convergent in time.

Taking the famous FFT, both sides of (1) in spatial variable x , (1) can be written as the following ordinary differential equations:

$$\frac{\partial}{\partial t} \mathbb{F}_x(\mathbf{u}(x, t)) = -\left(id_1(t) + |\kappa|^\alpha d_2(t)\right) \mathbb{F}_x(\mathbf{u}(x, t)) + id_3(t) \mathbb{F}_x(|\mathbf{u}(x, t)|^2 \mathbf{u}(x, t)). \quad (2)$$

For the convenience of expression, we denote

$$\zeta(t, \hat{\mathbf{u}}) = -\left(|\kappa|^\alpha d_2(t) + id_1(t)\right) \mathbb{F}_x(\mathbf{u}(x, t)) + id_3(t) \mathbb{F}_x\left(\mathbf{u}(x, t) |\mathbf{u}(x, t)|^2\right). \quad (3)$$

Equation (2) is converted to the following form:

$$\begin{cases} \frac{d\hat{\mathbf{u}}}{dt} = \zeta(t, \hat{\mathbf{u}}), \\ \hat{\mathbf{u}}(\kappa, 0) = \hat{\mathbf{u}}_0. \end{cases} \quad (4)$$

We then solve Equation (4) with the following conspicuous RKM, which has the following form:

$$\begin{cases} \hat{\mathbf{u}}_{n+1} = \hat{\mathbf{u}}_n + \frac{h}{6}(r_1 + 4r_2 + r_3), \\ r_1 = \zeta(t_n, \hat{\mathbf{u}}_n), \\ r_2 = \zeta(t_n + \frac{1}{2}h, \hat{\mathbf{u}}_n + \frac{1}{2}hr_1), \\ r_3 = \zeta(t_n + h, \hat{\mathbf{u}}_n - hr_1 + 2hr_2), \end{cases} \quad (5)$$

where h is time step-size. Three-order RKM has the following properties.

Property 1. If this incremental function $\Psi(\hat{\mathbf{u}}, t, h) = \frac{1}{6}(\zeta(t_n, \hat{\mathbf{u}}_n) + 4\zeta(t_n + \frac{1}{2}h, \hat{\mathbf{u}}_n + \frac{1}{2}hr_1) + \zeta(t_n + h, \hat{\mathbf{u}}_n - hr_1 + 2hr_2))$ is continuous on time domain $0 \leq t \leq T$, variable $-\infty \leq \hat{\mathbf{u}} \leq \infty$, and satisfies the famous Lipschitz condition about $\hat{\mathbf{u}}$, $|\Psi(t, \hat{\mathbf{u}}, h) - \Psi(t, \tilde{\hat{\mathbf{u}}}, h)| \leq L_\Psi |\hat{\mathbf{u}} - \tilde{\hat{\mathbf{u}}}|$, then the present numerical solution of Equation (4) is well-posed. Here, compelling L_Ψ is called a Lipschitz coefficient.

Property 2. If function $\Psi(t, \hat{\mathbf{u}}, h)$ of $\hat{\mathbf{u}}$ on $-\infty \leq \hat{\mathbf{u}} \leq \infty$ satisfies the famous Lipschitz condition. Let $E_n = \hat{\mathbf{u}}_n - \hat{\mathbf{u}}(t_n)$, and \mathbf{C} is a constant; we can obtain the following error estimation form: $|E_n| \leq \frac{\mathbf{C}h^3}{L_\Psi} (e^{L_\Psi T} - 1) + e^{L_\Psi T} |E_0|$.

Property 3. If function $\Psi(t, \hat{\mathbf{u}}, h)$ of $\hat{\mathbf{u}}$ on $-\infty \leq \hat{\mathbf{u}} \leq \infty$ satisfies the famous Lipschitz condition, then the present method is stable and convergent.

Finally, the numerical solution of the fractional-in-space variable coefficients NLSE with the unbounded domain can be obtained by applying the inverse FFT. In the actual calculation, we do not directly use the definition of the Fourier transform to calculate but call the fftshift function and ifftshift function to calculate. In general, the spectral methods are far more accurate than the finite difference method. Due to the continuous development of FFT technology, spectral methods are less and less computational, which is generally very cost-effective. Especially for the three-dimensional problem, the finite difference method must set enough grid points to increase the amount of calculation, while the spectral method generally does not need to take too many terms to obtain a more high-precision solution. Therefore, spectral methods are widely used in the computation of complex flow fields in fluid mechanics.

3. Numerical Experiment

Firstly, we determine the effectiveness of the proposed method by comparing the present numerical solution and exact solution. Then, the FSPB is investigated for the fractional-in-space NLSE with a variable coefficient on the large time-spatial domain. In the numerical simulation, the spatial domain is $[-L/2, L/2]$ and the spatial step size $h = L/N$, and N is a natural number.

Experiment 1. Select $d_1(t) = 0$, $d_2(t) = \frac{\cos t}{2}$, $d_3(t) = \frac{\cos t}{3 + \sin t}$ in Equation (1), and

$$\mathbf{u}(x, 0) = \frac{1}{\sqrt{3}} \sec\left(\frac{x}{3}\right) \exp\left(\frac{i(1-x^2)}{6}\right), \quad (6)$$

when $\alpha = 2$, in this case, the Equation (1) has the following exact solution

$$u(x, t) = \frac{1}{\sqrt{3 + \sin t}} \sec\left(\frac{x}{3 + \sin t}\right) \exp\left(\frac{i(1 - x^2)}{2(3 + \sin t)}\right). \tag{7}$$

Firstly, we determine the validity and precision of the proposed method by comparing the present numerical solution and its exact solution. The logarithmic of some absolute errors on the large time-spatial domain of Experiment 1 is shown in Figures 1 and 2.

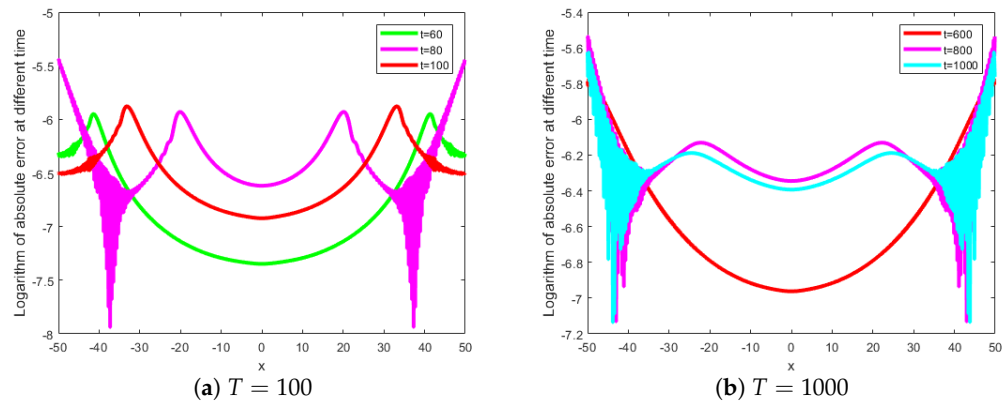


Figure 1. Logarithmic of the absolute error on different long-time domains of Experiment 1 ($\alpha = 2$).

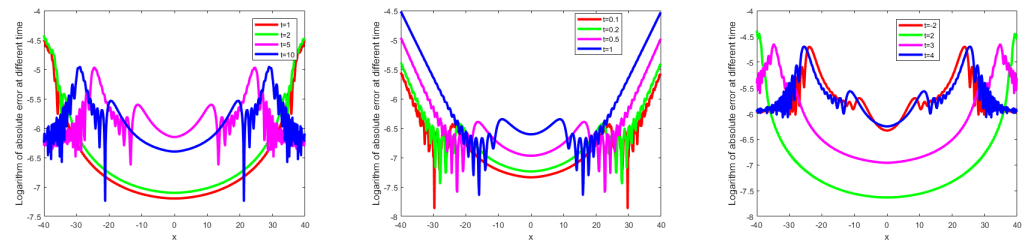


Figure 2. Logarithmic of the absolute error on different long-time domains of Experiment 1 ($\alpha = 2$, $h = 0.1, L = 80, N = 512$).

Figures 1 and 2 show that the present method at the large time-spatial domain has high accuracy. Then, the FSPB is numerically simulated at different α and different large time-spatial domains for the fractional-in-space variable coefficient NLSE.

Figure 3 shows some FSPBs at different fractional derivatives α and different time domains for Experiment 1. Figure 4 shows FSPB of imaginary part and real part and modulus at fractional derivative $\alpha = 1.6$ for Experiment 1. Figure 5 shows FSPB of real part and modulus at fractional derivative $\alpha = 1.8$ for Experiment 1. From Figures 3–5, we show the influences of the fractional derivatives α on the fractal wave propagation by the numerical simulation results. From Figures 3–5, we can see that the number of soliton spikes does not change and the peak height changes. The propagation of fractal soliton waves is investigated for the space NLSE with variable coefficients. The fractional derivative does not affect the wave, and as time goes on, the wave keeps propagating forward.

Next, in Equation (1), select $d_1(t) = 0, d_2(t) = \frac{\cos t}{2}, d_3(t) = \frac{\cos t}{\sin t + 3}$, and the initial-value condition is $u(x, 0) = \sec(6 + 2x) \exp(i(x - 2))$. We find some novel FSPBs at the large time-spatial domain for the fractional-in-space NSE, and these novel FSPBs are shown in Figures 6 and 7.

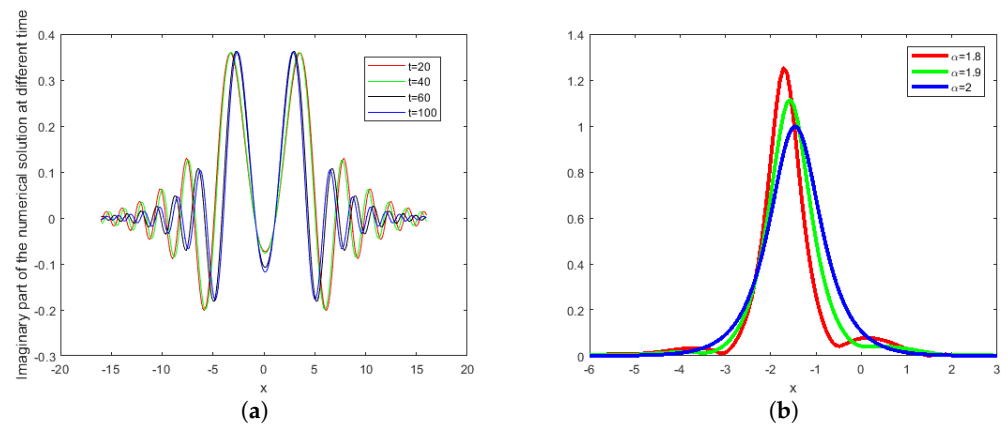


Figure 3. Simulation result of FSPB for Experiment 1 on different α and different long-time domains. (a) $\alpha = 1.6$. (b) Modulus at different fractional derivatives and $t = 200$.

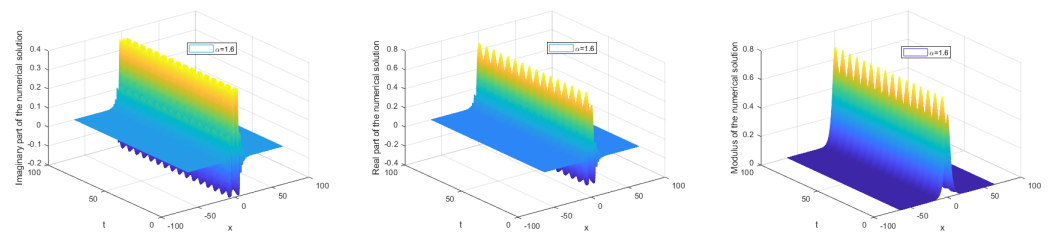


Figure 4. Simulation result of FSPB for Experiment 1 at $\alpha = 1.6$.

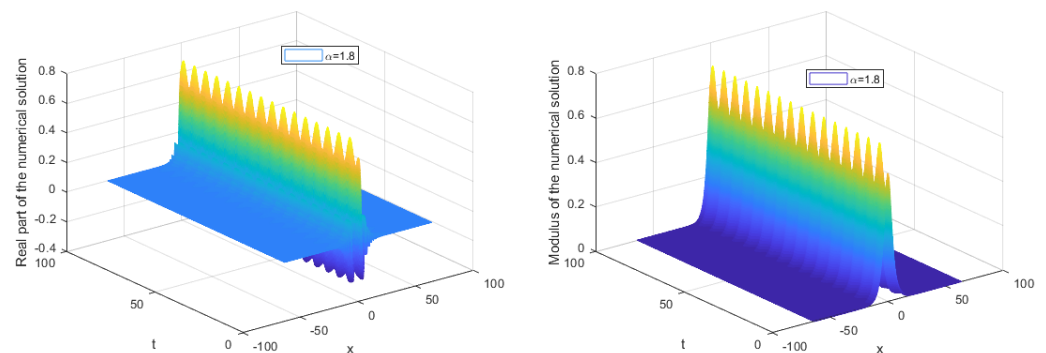


Figure 5. Simulation result of FSPB for Experiment 1 at $\alpha = 1.8$.

We find that this novel fractal soliton wave propagation behavior travels in one direction, that the wave shape does not change with time, and that these traveling waves are divided into a small region of space. These fractal waves roll forward, maintaining their shape and speed as they go.

Finally, the present method is extended for solving the three-dimensional fractional-in-space NLSE with a large time-spatial domain. We use the real part of the numerical solution to draw an isosurface plot, and two isosurface plots are shown in Figure 8.

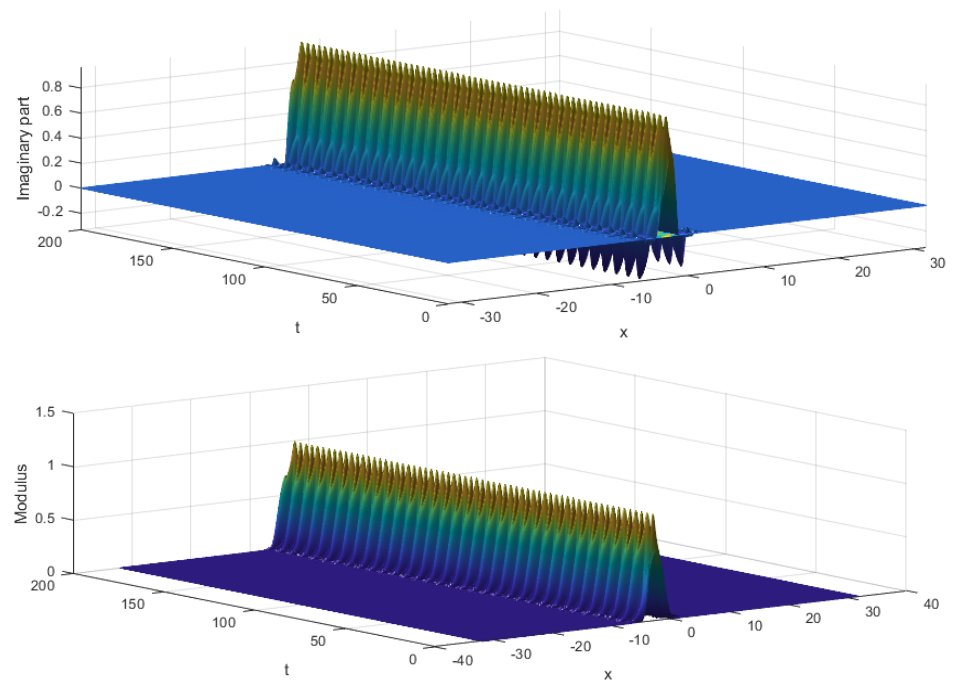


Figure 6. Simulation result of FSPB for Experiment 1 ($\alpha = 1.8, L = 64, N = 512, h = 0.01, T = 200$).

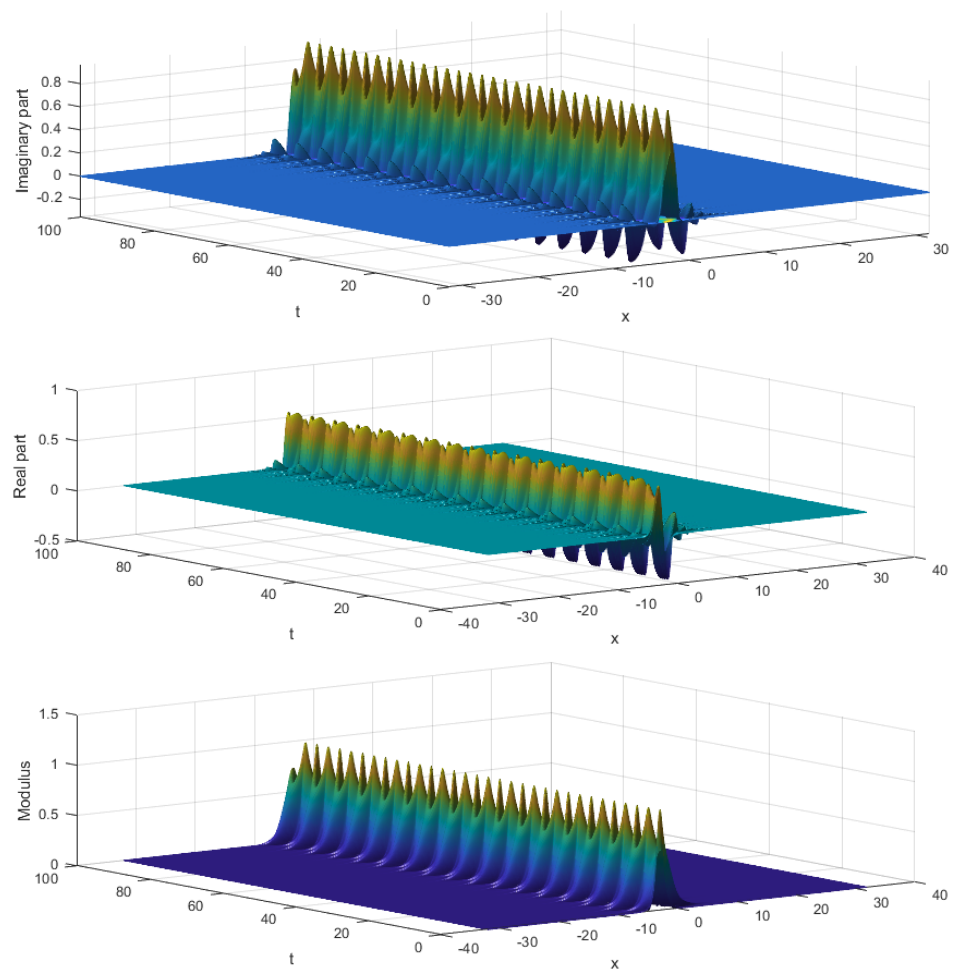


Figure 7. Simulation result of FSPB for Experiment 1 ($u(x,0) = \exp(i(x-2)) \sec(2x+6), \alpha = 2, L = 64, N = 512, h = 0.01, T = 100$).

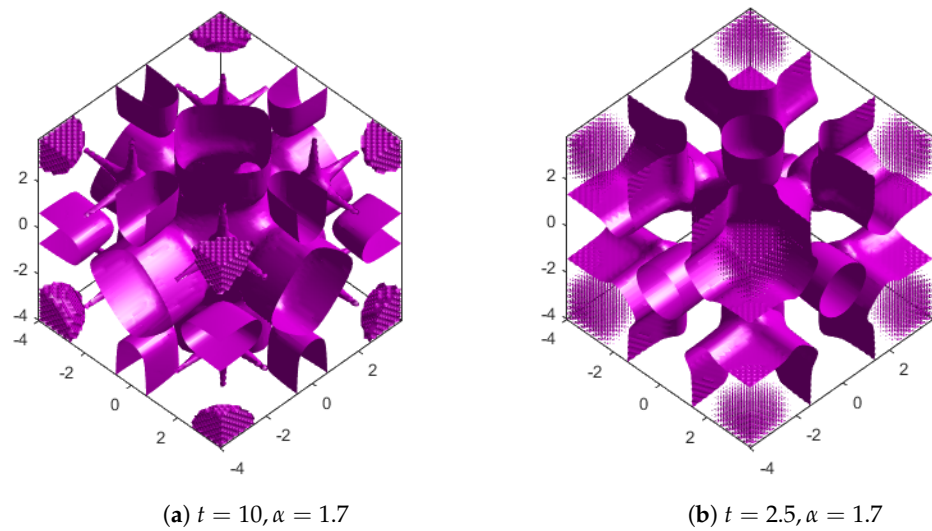


Figure 8. Simulation result of FSPB for Experiment 2.

Experiment 2. In Equation (1), Select $d_1(t) = \sin t$, $d_2(t) = \sin t$, $d_3(t) = 8 \sin t$. Some novel FSPB simulation results at the large time-spatial domain for the fractional-in-space NLSE with different $\mathbf{u}(x, 0)$ and α are shown in Figures 9–11.

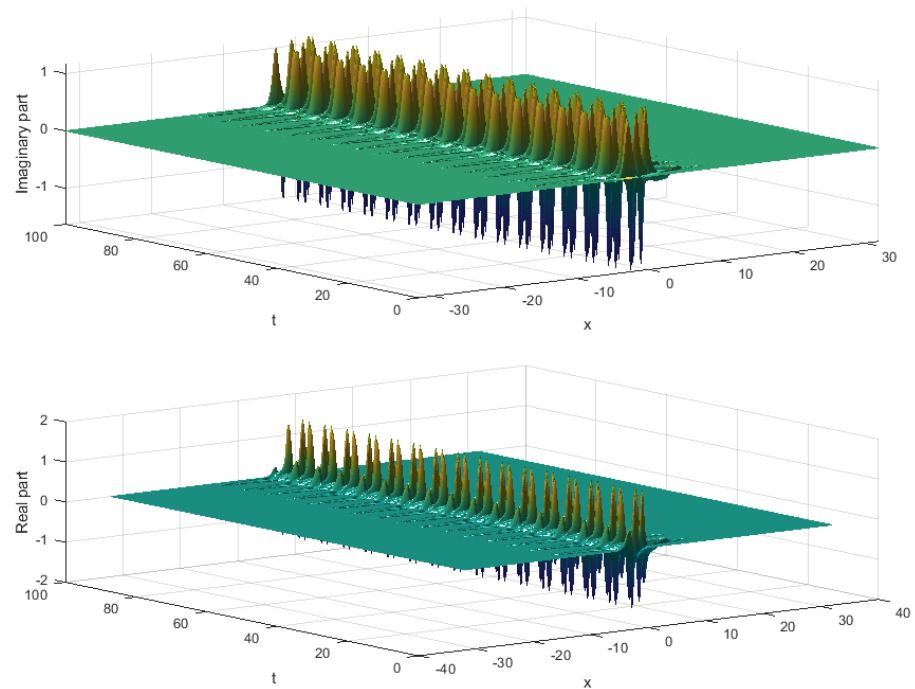


Figure 9. Simulation result of FSPB for Experiment 2 at $\mathbf{u}(x, 0) = \sec(6 + 2x) \exp(i(-2 + x))$, $\alpha = 1.6$, $L = 64$, $N = 512$, $h = 0.01$, $T = 100$.

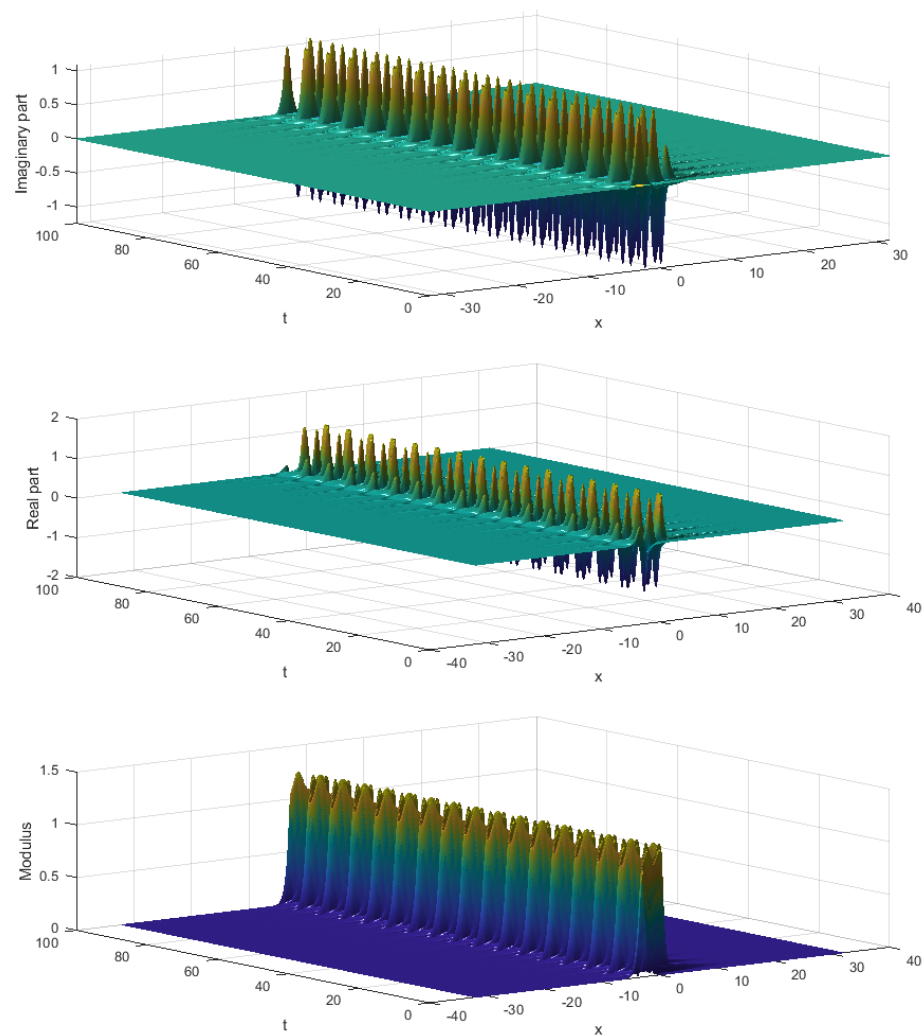


Figure 10. Numerical simulation result of FSPB for Experiment 2 at $\mathbf{u}(x, 0) = \sec(6 + 2x) \exp(i(-2 + x))$, $\alpha = 1.8$, $L = 64$, $N = 512$, $h = 0.01$, $T = 100$.

Figures 10 and 11 compare the FSPB under three initial-value conditions. Figures 9 and 10 compare the fractal soliton propagation behavior of the NLSE under two fractional derivatives $\alpha = 1.6, 1.8$. We find that these fractal soliton waves travel in one direction, that the wave shape does not change with time, and that these fractal soliton waves are in a small region of space. The fractional derivative does not affect the soliton wave, and as time goes on, the wave keeps propagating forward. The fractional derivative affects the shape of the soliton wave.

Table 1 shows the simulation results of FSPB for Experiment 2 at $\mathbf{u}(x, 0) = \frac{1}{\sqrt{3}} \sec\left(\frac{x}{3}\right) \exp\left(\frac{i(-1+x^2)}{6}\right)$, and different α . Table 2 shows the simulation results of FSPB for Experiment 2 under three initial conditions.

From Tables 1 and 2 and Figures 9–12, we further find that these FSPBs are in one direction, that the wave shape does not change with time, and that these fractal soliton waves are divided into a small region of space. These fractal waves roll forward, maintaining their shape and speed as they move forward.

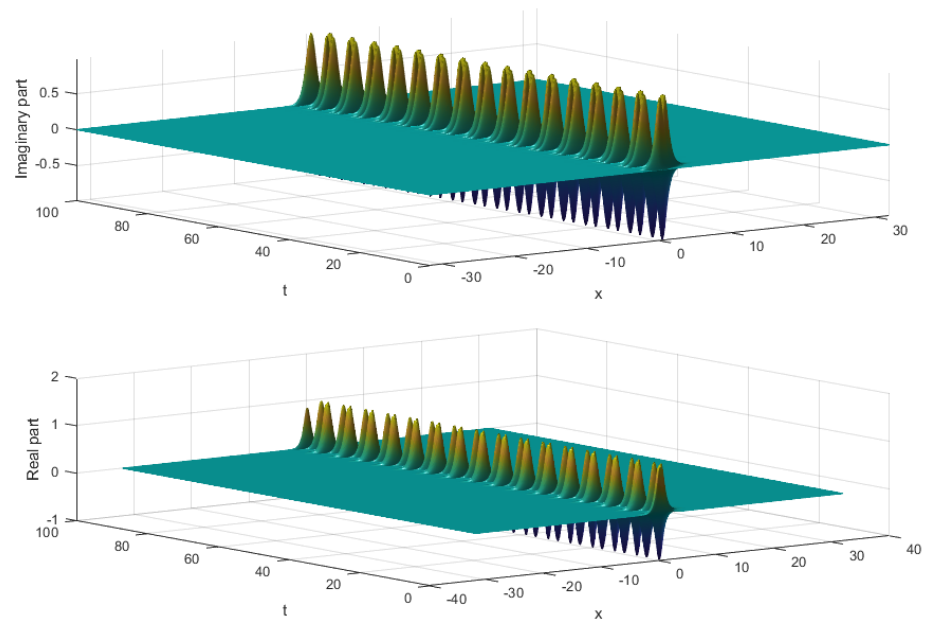


Figure 11. Simulation result of FSPB of Experiment 2 at $u(x,0) = \sec(2x)$ when $\alpha = 2, L = 64, N = 512, h = 0.01, T = 100$.

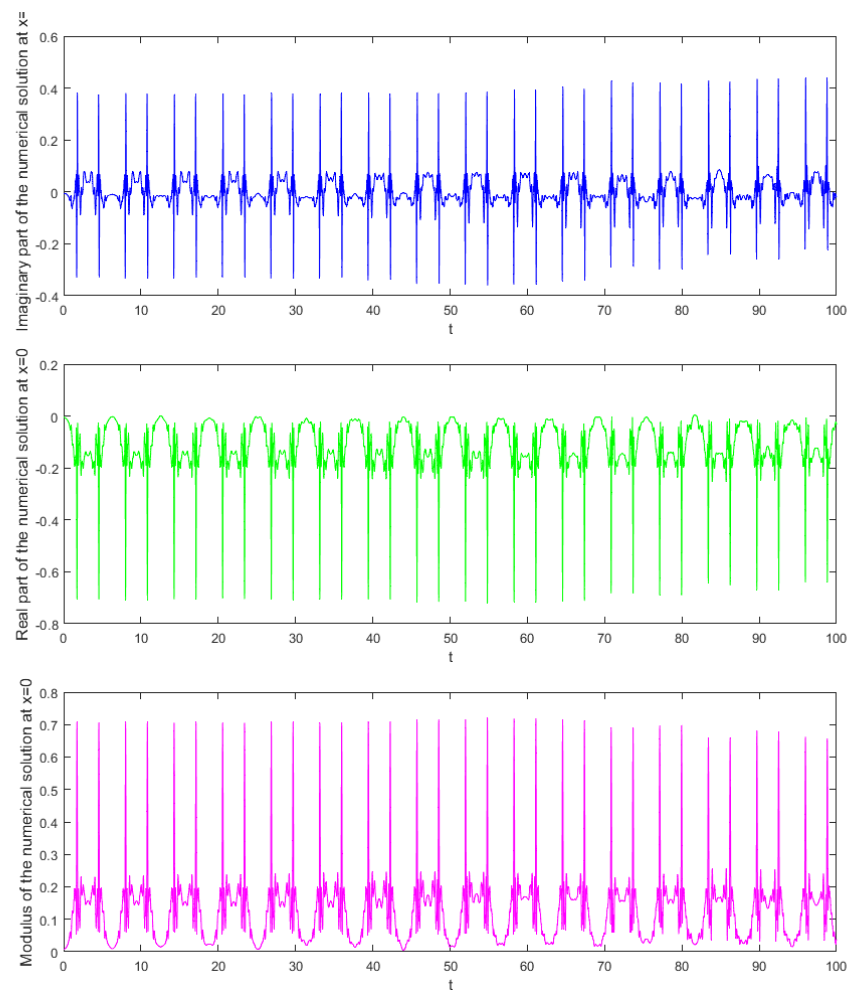


Figure 12. Simulation result for Experiment 2 at $\alpha = 1.2, x = 0, u(x,0) = \sec(6 + 2x) \exp(i(-2 + x)), L = 64, N = 512, h = 0.01, T = 100$.

Table 1. Simulation result of FSPB of Experiment 2 at $\alpha = 0.2, 1.2, 2$, $u(x, 0) = \frac{1}{\sqrt{3}} \sec\left(\frac{x}{3}\right) \exp\left(\frac{i(x^2-1)}{6}\right)$, $L = 64, N = 512, h = 0.01, T = 100$.

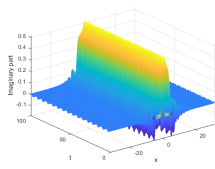
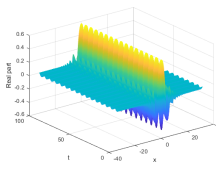
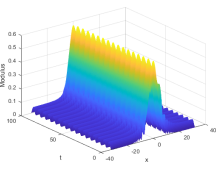
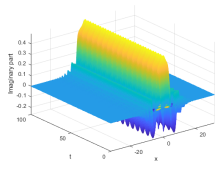
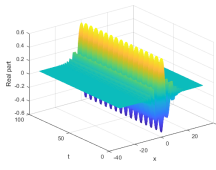
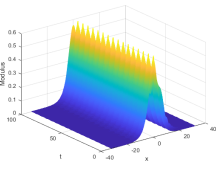
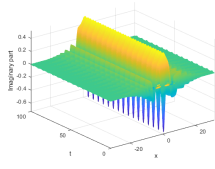
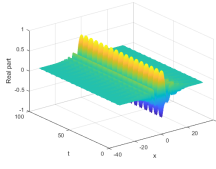
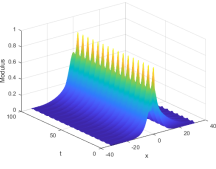
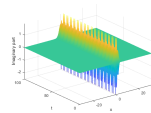
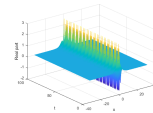
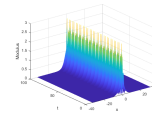
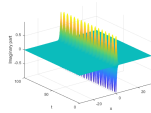
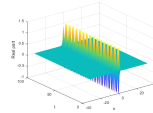
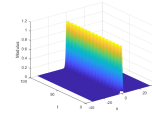
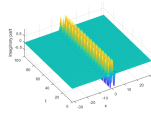
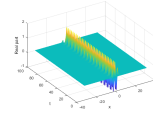
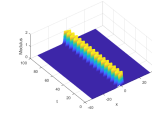
α	Imaginary Part	Real Part	Modulus
$\alpha = 0.2$			
$\alpha = 1.2$			
$\alpha = 2$			

Table 2. Simulation result of FSPB of Experiment 1 at three initial conditions when $\alpha = 2, L = 64, N = 512, h = 0.01, T = 100$.

Initial Condition	Imaginary Part	Real Part	Modulus
$\sec(-0.5x)$			
$\sec(-2x)$			
$\sec(6 + 2x) \exp(i(-2 + x))$			

4. Conclusions

In this paper, we observe how the solitary waves of the fractional-in-space NLSE with a variable coefficient change as the Laplacian operator changes and different initial conditions change. Some novel fractal solitary wave propagation behaviors of the fractional-in-space NLSE are shown. We find that these novel traveling waves travel in one direction, that the wave shape does not change with time, and that these traveling waves are in a small region of space. The influences of the fractional derivative α on the fractal wave propagation are shown through the numerical simulation. The fractional derivative does not affect the wave, and as time goes on, the wave keeps propagating forward. The fractional derivative affects the shape of the wave. It should be noted that how to ensure that the boundary conditions have little effect on the whole, or that the value at the boundary is always a specific constant, is a problem worth thinking about.

Author Contributions: Conceptualization, F.T. and Y.W.; Methodology and software, F.T. and Z.L.; Data curation, formal analysis, and funding acquisition, Y.W. and Z.L.; Validation, F.T. and Y.W.; Writing-original draft and writing-review and editing, F.T. and Y.W. All authors have read and agreed to the published version of the manuscript.

Funding: This paper is supported by doctoral research start-up fund of Inner Mongolia University of Technology (DC2300001252).

Data Availability Statement: The data used to support the findings of this study are available from the corresponding author upon request.

Conflicts of Interest: The authors declare that there are no conflicts of interest regarding the publication of this article.

References

- Hu, Y.; Kallianpur, G. Schrödinger equations with fractional Laplacians. *Appl. Math. Optim.* **2000**, *42*, 281–290. [\[CrossRef\]](#)
- Guo, X.; Xu, M. Some physical applications of fractional Schrödinger equation. *J. Math. Phys.* **2006**, *47*, 082104. [\[CrossRef\]](#)
- Guo, B.; Han, Y.; Xin, J. Existence of the global smooth solution to the period boundary value problem of fractional nonlinear Schrödinger equation. *Appl. Math. Comput.* **2008**, *204*, 468–477. [\[CrossRef\]](#)
- Li, C.P.; Yi, Q.; Chen, A. Finite difference methods with non-uniform meshes for nonlinear fractional differential equations. *J. Comput. Phys.* **2016**, *316*, 614–631. [\[CrossRef\]](#)
- Peranich, L. A finite difference scheme for solving a nonlinear Schrödinger equation with a linear damping term. *J. Comput. Phys.* **1987**, *68*, 501–505. [\[CrossRef\]](#)
- Ciegis, R.; Pakalnyte, V. The finite difference scheme for the solution of weakly damped non-linear Schrödinger equation. *Int. J. Appl. Math. Comput. Sci.* **2001**, *8*, 127–134.
- Liu, Q.; Zeng, F.H.; Li, C.P. Finite difference method for time-space-fractional Schrödinger equation. *Int. J. Comput. Math.* **2015**, *92*, 1439–1451. [\[CrossRef\]](#)
- Zhang, Y.; Feng, X.; Qian, L. A second-order $L_2 - 1_\sigma$ difference scheme for the non-linear time-space fractional Schrödinger equation. *Commun. Nonlinear Sci. Numer. Simul.* **2024**, *131*, 107839. [\[CrossRef\]](#)
- Liu, Y.; Maohua, R. Arbitrarily high-order explicit energy-conserving methods for the generalized nonlinear fractional Schrödinger wave equations. *Math. Comput. Simul.* **2024**, *216*, 126–144. [\[CrossRef\]](#)
- Yuan, W.Q.; Zhang, C.J.; Li, D.F. Linearized fast time-stepping schemes for time-space fractional Schrödinger equations. *Phys. D* **2023**, *454*, 133865. [\[CrossRef\]](#)
- Li, Z.; Chen, Q.; Wang, Y.; Li, X. Solving two-sided fractional super-diffusive partial differential equations with variable coefficients in a class of new reproducing kernel spaces. *Fractal Fract.* **2022**, *6*, 492. [\[CrossRef\]](#)
- Li, H.W.; Chen, L.L. Numerical solution of nonlinear Schrödinger equation with damping term on unbounded domain. *Appl. Math. Lett.* **2024**, *148*, 108893. [\[CrossRef\]](#)
- Cai, J.; Chen, J.; Efficient dissipation-preserving approaches for the damped nonlinear Schrödinger equation. *Appl. Numer. Math.* **2023**, *183*, 173–185. [\[CrossRef\]](#)
- Li, C.P.; Li, Z.Q. The blow-up and global existence of solution to Caputo-Hadamard fractional partial differential equation with fractional Laplacian. *J. Nonlinear Sci.* **2021**, *31*, 80. [\[CrossRef\]](#)
- Guo, S.; Yan, W.; Li, C.; Mei, L. Dissipation-preserving rational spectral-Galerkin method for strongly damped nonlinear wave system involving mixed fractional Laplacians in unbounded domain. *J. Sci. Comput.* **2022**, *93*, 53. [\[CrossRef\]](#)
- Bashan, A.; Yagmurlu, N.M.; Ucar, Y.; Esen, A. An effective approach to numerical soliton solutions for the Schrödinger equation via modified cubic B-spline differential quadrature method. *Chaos Solitons Fractals* **2017**, *100*, 45–56. [\[CrossRef\]](#)
- Braun, M. Numerical solution of the one dimensional Schrödinger equation using a basis set of scaled and shifted sinc functions on a finite interval. *J. Comput. Appl. Math.* **2023**, *429*, 115224. [\[CrossRef\]](#)
- Kulagin, A.E.; Shapovalov, A.V. A semiclassical approach to the nonlinear Schrödinger equation with a non-Hermitian term. *Mathematics* **2024**, *12*, 580. [\[CrossRef\]](#)
- Aldhafeeri, A.; Al Nuwairan, M. Bifurcation of some novel wave solutions for modified non-linear Schrödinger equation with time M-fractional derivative. *Mathematics* **2023**, *11*, 1219. [\[CrossRef\]](#)
- Liaqat, M.I.; Akgül, A. A novel approach for solving linear and nonlinear time-fractional Schrödinger equations. *Chaos Solitons Fractals* **2022**, *162*, 112487. [\[CrossRef\]](#)
- He, J.H.; Jiao, M.L.; He, C.H. Homotopy perturbation method for fractal duffing oscillators with arbitrary conditions. *Fractals* **2022**, *30*, 2250165. [\[CrossRef\]](#)
- Zhang, H.; Jiang, X.Y.; Wang, C.; Chen, S. Crank-Nicolson Fourier spectral methods for the space fractional nonlinear Schrödinger equation and its parameter estimation. *Int. J. Comput. Math.* **2019**, *96*, 238–263. [\[CrossRef\]](#)
- Abdolabadi, F.; Zakeri, A.; Amiraslani, A. A split-step Fourier pseudo-spectral method for solving the space fractional coupled nonlinear Schrödinger equations. *Commun. Nonlinear Sci. Numer. Simul.* **2023**, *120*, 107150. [\[CrossRef\]](#)

24. Han, C.; Wang, Y.L.; Li, Z.Y. A high-precision numerical approach to solving space fractional Gray-Scott model. *Appl. Math. Lett.* **2022**, *125*, 107759. [[CrossRef](#)]
25. Bai, D.M.; Wang, J.L. The time-splitting Fourier spectral method for the coupled Schrödinger-Boussinesq equations. *Commun. Nonlinear Sci. Numer. Simul.* **2012**, *17*, 1201–1210. [[CrossRef](#)]
26. Liang, X.; Khaliq, A.Q.M. An efficient Fourier spectral exponential time differencing method for the space-fractional nonlinear Schrödinger equations. *Comput. Math. Appl.* **2018**, *75*, 4438–4457. [[CrossRef](#)]
27. Farag, N.G.A.; Eltanboly, A.H.; El-Azab, M.S.; Obayya, S.S.A. Numerical solutions of the (2+1)-dimensional nonlinear and linear time-dependent Schrödinger equations using three efficient approximate schemes. *Fractal Fract.* **2023**, *7*, 188. [[CrossRef](#)]
28. Cheng, B.R.; Guo, Z.H. Regularized splitting spectral method for space-fractional logarithmic Schrödinger equation. *Appl. Numer. Math.* **2021**, *167*, 330–355. [[CrossRef](#)]
29. Han, C.; Wang, Y.L.; Li, Z.Y. Novel patterns in a class of fractional reaction-diffusion models with the Riesz fractional derivative. *Math. Comput. Simul.* **2022**, *202*, 149–163.
30. Ning, J.; Wang, Y.L. Fourier spectral method for solving fractional-in-space variable coefficient KdV-Burgers equation. *Indian J. Phys.* **2023**. [[CrossRef](#)]

Disclaimer/Publisher’s Note: The statements, opinions and data contained in all publications are solely those of the individual author(s) and contributor(s) and not of MDPI and/or the editor(s). MDPI and/or the editor(s) disclaim responsibility for any injury to people or property resulting from any ideas, methods, instructions or products referred to in the content.